
INFLUENCE OF LOCAL FIELD ON SPONTANEOUS LIGHT EMISSION BY NANOPARTICLES

I. IEZHOKIN, O. KELLER¹, V. LOZOVSKI

UDC 535
© 2009

Taras Shevchenko Kyiv National University, Faculty of Radiophysics
(2, Academician Glushkov Ave., Kyiv 03127, Ukraine; e-mail: ejik_gradx@mail.ru),

¹Institute of Physics and Nanotechnology, Aalborg University
(4, Skjernvej, Bld. A, Aalborg Øst 9220, Denmark)

A self-consistent approach based on the local-field concept has been proposed to calculate the direction patterns of light emission by nanoparticles with various shapes. The main idea of the method consists in constructing self-consistent equations for the electromagnetic field at any point of the system. The solution of the equations brings about relationships between the local field at an arbitrary point in the system and the external long-wave field via the local-field factor. The latter connects the initial moment of optical dipole transition per system volume unit and the effective dipole moment of transition that takes local-field effects into account. The effective dipole moment depends on the particle shape and size. Therefore, dipole radiation depends on those parameters too. The direction patterns of light emission by cubic particles have been calculated. The particles have been demonstrated to interact as almost point dipoles at distances that exceed their linear dimensions. This fact can be used to substantiate applications of the dipole approximation to studying the optical properties of submonolayer molecular coatings.

1. Introduction

The development of modern technologies gave rise not only to the mastering of the nanometer scale in electronics and the elaboration of essentially new electronic devices, which stimulated the transition from micro- to nanoelectronics [1–4], but also to the emergence of new – subwave – optics, the so-called near-field optics [5–7]. The rapid development of this new branch of optics has been continuing for last two decades. Within this time period, the progress in near-field optics has converted the application of optical scanning microscopy into a routine experimental technique for studying local field distributions in nanosystems [8–10]. Nowadays, the researches of local

field distributions serve merely scientific [11–13] and rather utilitarian purposes [14–16]. For instance, they are applied to the development of photonic crystal devices for optical information processing. On the other hand, the near-field optics gave an impetus to the development of fundamental researches in quantum electrodynamics [17–19], which resulted, e.g., in a revision of the problem of light emission by material objects.

In this connection, works [19–21] of one of the authors of this article (O.K.) can be exemplified. A detailed consideration of the process of photon emission by an excited atom carried out in those works demonstrated, in particular, that the excited state of the system “atom + electromagnetic field” is characterized by a complicated structure of the electric field, the latter possessing both the longitudinal and transverse components. In addition, the dependence of the energy of the electromagnetic field transverse component on the oscillation number is periodic, and the difference between the electromagnetic field energy and the photon energy $\hbar\omega$ is less than ten percent even for the tenth period of oscillations. Hence, the emitted photon carries information about the particle that has generated it. But, in those works, details of photon emission processes were studied in the point-like emitter approximation. In this connection, a question arises: How do the dimensions and the shape of the emitting particle affect the process of photon emission? Really, it is known that, in optics, the optical properties of mesoparticles are governed to a great extent by the particle’s dimensions and shape [22–25]. It is clear that a similar situation should be observed, when studying the processes of radiation emission by

an extended particle. This work aims at studying the influence of the particle's extension on its light radiation properties.

The spontaneous photon emission by a particle can be regarded as the appearance of a radiation induced by the electron current that arises in the particle owing to electron transitions. In this case, the influence of the particle's extension on the emission process can be divided into two components. First, electron transitions occur differently at different particle sites. That is, the fields that are induced by elementary currents should be integrated over the particle's volume. Second, the process of current formation undergoes the action of a self-field that the currents invoke. This local-field effect can bring about, for example, a shift of electron energy levels in the particle (the effect is similar to the Lamb shift in nuclear physics). To take the influence of the self-field on the formation of currents in the particle into account, this local field has to be calculated. The calculations of local fields in the near-field physics are carried on by solving a self-consistent problem. This procedure is reduced to finding the solutions of the Lippmann–Schwinger equation.

2. Local Field at Light Emission by Mesoparticles with Various Shapes

To study the influence of local field effects on the processes of photon emission by nanoparticles with various shapes, we have to determine how the energy flux density of the electromagnetic field emitted by the particle is formed. This means that we have to calculate the Poynting's vector. For this purpose, let us determine how the dipole moment of an optical transition in the particle becomes "dressed" owing to the electrodynamic interaction, which is the origin of radiation emission.

The local field satisfies the self-consistent Lippmann–Schwinger equation [5–8]

$$E_i(\mathbf{R}, \omega) = E_i^{(I)}(\mathbf{R}, \omega) - i\omega\mu_0 \int_V d\mathbf{R}' G_{ij}(\mathbf{R}, \mathbf{R}', \omega) J_j(\mathbf{R}', \omega), \quad (1)$$

where $G_{ij}(\mathbf{R}, \mathbf{R}', \omega)$ is the photon propagator of the medium that the emitting particle is located in. As was shown in works [26–28], the solution of Eq. (1) can be expressed in the form

$$E_i(\mathbf{R}, \omega) = E_i^{(I)}(\mathbf{R}, \omega) -$$

¹Note that the material equation connects the local current and the local field by means of the material susceptibility: $J_i(\mathbf{R}, \omega) = -i\omega\chi_{il}(\omega)E_l(\mathbf{R}, \omega)$.

$$-i\omega\mu_0 \int_V d\mathbf{R}' G_{ij}(\mathbf{R}, \mathbf{R}', \omega) X_{jl}(\mathbf{R}', \omega) E_i^{(I)}(\mathbf{R}', \omega), \quad (2)$$

where $X_{jl}(\mathbf{R}', \omega)$ is the tensor of effective susceptibility that couples the local current $J_i(\mathbf{R}, \omega)$ with the external (with respect to the particle) field $E_i^{(I)}(\mathbf{R}, \omega)$ by the relation¹

$$J_i(\mathbf{R}, \omega) = -i\omega X_{il}(\mathbf{R}, \omega) E_l^{(I)}(\mathbf{R}, \omega). \quad (3)$$

The effective susceptibility has a standard form of the linear response function [29],

$$X_{ij}(\mathbf{R}, \omega) = [(\chi_{ij}(\omega))^{-1} + \tilde{S}_{ji}(\mathbf{R}, \omega)]^{-1} = \chi_{il}(\omega) [\delta_{jl} + S_{ji}(\mathbf{R}, \omega)]^{-1}, \quad (4)$$

where the self-energy part $S_{ij}(\mathbf{R}, \omega)$ reads

$$S_{ji}(\mathbf{R}, \omega) = -i\omega\mu_0 \int_V d\mathbf{R}' G_{jl}(\mathbf{R}', \mathbf{R}, \omega) \chi_{li}(\omega). \quad (5)$$

Using the reciprocity theorem [30], the latter can be rewritten in the form

$$S_{ji}(\mathbf{R}, \omega) = -i\omega\mu_0 \int_V d\mathbf{R}' G_{jl}(\mathbf{R}, \mathbf{R}', \omega) \chi_{li}(\omega). \quad (6)$$

The local field factor, which connects the self-consistent field at any point of the system [5] with the external field by the relation

$$E_i(\mathbf{R}, \omega) = L_{il}(\mathbf{R}, \omega) E_l^{(0)}(\mathbf{R}, \omega),$$

looks like

$$L_{ij}(\mathbf{R}, \omega) = \delta_{ij} - i\omega\mu_0 \int_V d\mathbf{R}' G_{jl}(\mathbf{R}, \mathbf{R}', \omega) X_{li}(\mathbf{R}', \omega). \quad (7)$$

Hence, the problem of finding the local field in the system is reduced to calculating the local field factor. In its turn, in order to determine the local field of a photon emitted by a mesoparticle with a definite shape, it is necessary to calculate the effective susceptibility of the particle. The latter parameter evidently depends on the substance the particle is made of (i.e. on the local field response function χ) and on the particle's dimensions and shape, as follows directly from formula (4).

3. Local Field of Light Emitted by a Quantum Dot

It is clear that a particle with spatial quantization (a quantum dot) emits a photon in a little different manner than a mesoparticle does (mesoparticle is such a particle, the linear dimensions of which are, on the other hand, small enough for the local field effects to substantially influence its properties, but, on the other hand, are not too small for the effects of spatial quantization to manifest themselves). As was elucidated in the previous section, the determination of the local field emitted by a mesoparticle is reduced to the calculation of the tensor of its effective susceptibility. In this section, we show that a similar approach can be applied to the analysis of the photon emission by a quantum dot.

For the sake of definiteness, consider a quantum dot as a potential box with infinitely high potential walls. This means that particle's electrons move in a region confined by infinitely high potential barriers, i.e. the potential energy is given by the expression

$$V = \begin{cases} 0, & \text{inside a particle,} \\ \infty, & \text{outside it.} \end{cases} \quad (8)$$

If the linear dimensions of a rectangular quantum dot are L_x , L_y , and L_z , electrons move in the region given by the inequalities $-L_x/2 \leq x \leq L_x/2$, $-L_y/2 \leq y \leq L_y/2$, and $-L_z/2 \leq z \leq L_z/2$. For potential (8), the wave function of electrons in the quantum well is [31,32]

$$\begin{aligned} \Psi_{n_1, n_2, n_3}(x, y, z) &= \sqrt{\frac{8}{L_x L_y L_z}} \sin \left[\frac{\pi n_1}{L_x} \left(x + \frac{L_x}{2} \right) \right] \times \\ &\times \sin \left[\frac{\pi n_2}{L_y} \left(y + \frac{L_y}{2} \right) \right] \sin \left[\frac{\pi n_3}{L_z} \left(z + \frac{L_z}{2} \right) \right], \end{aligned} \quad (9)$$

where $n_i = 0, 1, 2, \dots (i = 1, 2, 3)$ are the quantum numbers. The energy corresponding to the (n_1, n_2, n_3) quantum state of an electron is

$$\varepsilon_{n_1, n_2, n_3} = \frac{\hbar^2 \pi^2}{2 \cdot m^*} \left(\frac{n_1^2}{L_x} + \frac{n_2^2}{L_y} + \frac{n_3^2}{L_z} \right). \quad (10)$$

The electrodynamic properties of such a quantum dot are known to be governed by the currents that arise due to transitions between the ground and excited states [33–36]. To determine the effective susceptibility (or – directly – the local field factor), let us take advantage of a procedure developed in works [35,36]. Note that the electric current density induced by electron transitions

in the quantum dot is coupled with the electric field by the nonlocal relation

$$J_k(\mathbf{R}, \omega) = \int_V \sigma_{kl}(\mathbf{R}, \mathbf{R}', \omega) E_l(\mathbf{R}', \omega) d\mathbf{R}', \quad (11)$$

where

$$\sigma_{kl}(\mathbf{R}, \mathbf{R}', \omega) = -\frac{i}{\mu_0 \omega} \sum_{\alpha} a_{\alpha}(\omega) j_k^{\alpha 0}(\mathbf{R}) j_l^{0\alpha}(\mathbf{R}') \quad (12)$$

is the electroconductivity tensor, $j_k^{\alpha 0}(\mathbf{R})$ and $j_l^{0\alpha}(\mathbf{R}')$ are the current densities of the transition between the ground energy level “0” and the level “ α ” [33]:

$$j_i^{0\alpha} = -\frac{e\hbar}{2im} [(\psi^{\alpha})^* \nabla_i \psi^0 - \psi^0 (\nabla_i \psi^{\alpha})^*], \quad (13)$$

ψ^0 is the wave function of the ground state, and ψ^{α} is the wave function of the excited state α . The quantity a_{α} is given by the expression

$$a_{\alpha}(\omega) = 2\mu_0 \frac{E_{\alpha} - E_0}{\hbar^2(\omega + i\nu)^2 - (E_{\alpha} - E_0)^2}, \quad (14)$$

where E_{α} is the energy of state α , and ν the relaxation frequency. Substituting expression (12) into the Lippmann–Schwinger equation (1), we obtain the equation for the self-consistent (local) field:

$$\begin{aligned} E_i(\mathbf{R}, \omega) &= E_i^{(0)}(\mathbf{R}, \omega) - \\ &- \sum_{\alpha} a_{\alpha}(\omega) F_i^{\alpha 0}(\mathbf{R}, \omega) \int_V d\mathbf{R}' j_l^{0\alpha}(\mathbf{R}') E_l(\mathbf{R}', \omega), \end{aligned} \quad (15)$$

where

$$F_i^{\alpha 0}(\mathbf{R}, \omega) = \frac{\mu_0}{\hbar} \int_V d\mathbf{R}' G_{ik}(\mathbf{R}, \mathbf{R}', \omega) j_k^{\alpha 0}(\mathbf{R}') \quad (16)$$

is the electromagnetic field at the point \mathbf{R} , which is induced by the current of the electron transition $\alpha \rightarrow 0$. Applying the integral operator $\int_V d\mathbf{R} j_i^{0\beta}$ to both parts of

Eq. (15), we obtain the system of algebraic equations

$$\sum_{\alpha} (\delta_{\alpha\beta} + a_{\alpha}(\omega) N^{\alpha\beta}(\omega)) \gamma^{0\alpha}(\omega) = \gamma_{(0)}^{\beta 0}(\omega), \quad (17)$$

where the variable

$$\gamma^{0\alpha}(\omega) = \int_V d\mathbf{R} j_i^{0\alpha}(\mathbf{R}) E_i(\mathbf{R}, \omega) \quad (18)$$

is to be determined. Hence, to find the local field factor, we obtained the system of algebraic equations (17), where the notation

$$N^{\alpha\beta}(\omega) = \int_V d\mathbf{R} j_i^{0\beta}(\mathbf{R}) F_i^{\alpha 0}(\mathbf{R}, \omega) = \\ = \iint_V d\mathbf{R} d\mathbf{R}' j_i^{0\beta}(\mathbf{R}) G_{ik}(\mathbf{R}, \mathbf{R}', \omega) j_i^{\alpha 0}(\mathbf{R}') \quad (19)$$

was introduced.

The external long-wave field is almost constant at distances compatible with the linear dimensions of the particle. Therefore, we can use the near-field approximation and put

$$\gamma_{(0)}^{0\beta}(\omega) = \int_V dR j_i^{0\beta}(\mathbf{R}) E_i^{(0)}(\mathbf{R}, \omega) = \tilde{\gamma}_i^{0\beta} E_i^{(0)}(\mathbf{R}, \omega). \quad (20)$$

The solution of the system of equations (17) can be written down in the form [33–37]

$$\gamma^{0\alpha}(\omega) = \frac{B^{\beta\alpha}}{\Delta} \tilde{\gamma}_i^{0\beta} E_i^{(0)}(\mathbf{R}, \omega), \quad (21)$$

where $B^{\beta\alpha}$ is the algebraic complement, and Δ is the determinant of the matrix $\delta_{\alpha\beta} + a_{\alpha} N^{\alpha\beta}$.

As a result, we obtain a relation between the local and external fields in the standard form

$$E_i(\mathbf{R}) = \Lambda_{il}(\mathbf{R}, \omega) E_l^{(0)}(\mathbf{R}) \quad (22)$$

with the local field factor

$$\Lambda_{ij}(\mathbf{R}, \omega) = \left\{ \delta_{ij} - \sum_{\alpha,\beta} a_{\alpha}(\omega) F_i^{\alpha 0}(\mathbf{R}, \omega) \frac{B^{\beta\alpha}}{\Delta} \tilde{\gamma}_j^{0\beta} \right\}. \quad (23)$$

Hence, we showed that the standard calculation procedure of a local field can be used in both considered cases of meso- and quantum particles. Knowing this field allows the energy flux of the field emitted by a particle to be calculated and, therefore, the radiation pattern to be determined.

4. Energy Flux of the Field Radiated by a Particle

The flux of electromagnetic field energy is known to be determined by the Poynting's vector

$$\mathbf{S} = \frac{1}{\mu_0} [\mathbf{E} \times \mathbf{H}]. \quad (24)$$

Let the source of the emitted field be the electron current \mathbf{I} localized in the particle. Then, the expressions for the magnetic and electric fields look like [38]

$$\mathbf{H}(\mathbf{R}) = -\frac{1}{c} \int_V d\mathbf{R}' [\mathbf{I} \times \mathbf{n}] \left(\frac{ik}{R_0} - \frac{1}{R_0^2} \right) e^{ikR_0}, \quad (25)$$

$$\mathbf{E}(\mathbf{R}) = \frac{i}{\omega} \int_V d\mathbf{R}' \left\{ \mathbf{I} \left(\frac{k^2}{R_0} + \frac{ik}{R_0^2} - \frac{1}{R_0^3} \right) + \right. \\ \left. + \mathbf{n}(\mathbf{nI}) \left(-\frac{k^2}{R_0} - \frac{3ik}{R_0^2} + \frac{3}{R_0^3} \right) \right\} e^{ikR_0}, \quad (26)$$

respectively, where

$$R_0 = \sqrt{(x-x')^2 + (y-y')^2 + (z-z')^2}$$

is the distance between an arbitrary point in the particle and a point of field observation, and \mathbf{n} is the unit vector that defines the direction to the latter. In the case where the point of observation is in the far-field zone, so that the electromagnetic wave front has already been formed, the vector \mathbf{n} defines a normal to the wave front at the point of observation.

In the framework of the problem concerned, the local field effects manifest themselves in a twofold manner. First, the current undergoes the self-field action, which modifies radiation emission conditions. For example, this effect gives rise to a shift of the lines of a radiating quantum dot (it is an analog of the Lamb shift in nuclear physics) [35–37]. How can the influence of the self-field on the current in the particle be taken into consideration? To understand this issue, suppose that the current arises, because a certain external field affects the particle. In this case, due to the self-field effects, the particle undergoes the action of the local field, which induces the current \mathbf{I} ,

$$\mathbf{I} = -i\omega\chi\mathbf{E}, \quad (27)$$

at an arbitrary point of the particle; χ is the tensor of the response to the local field. Since the local field is coupled with the external one by means of the local field factor (see formula (22)), $\mathbf{E} = \Lambda\mathbf{E}^{(0)}$, expression (27) yields

$$\mathbf{I} = -i\omega\chi\Lambda\mathbf{E}^{(0)}. \quad (28)$$

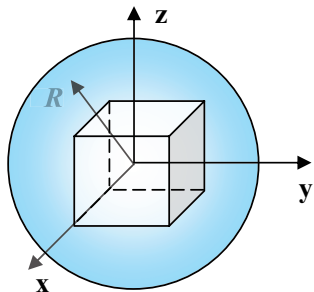


Fig. 1. Geometry of the problem

Let the current in a point-like object be equal to $\mathbf{e}I_0$, where \mathbf{e} is the unit vector along the current direction and the current is calculated without taking local-field effects into account. By comparing expressions (27) and (28), one can see that making allowance for the self-field effects is reduced to the multiplication of the current I_0 by the local-field factor. That is, the local current, which is the source of the radiated field, looks like

$$\mathbf{I} = \Lambda \mathbf{e} I_0. \quad (29)$$

Another way for the radiator extension to have an effect consists in that the contributions of all elementary currents to the field energy flux have to be summed up over all physically infinitesimal volumes of the particle. Thus, the Poynting's vector looks like

$$\mathbf{S}(\mathbf{R}) = (\omega I_0)^2 \left\{ \int_V d\mathbf{R}' \frac{1}{R_0^5} \left[-2(\Lambda \mathbf{z}) |\Lambda \mathbf{z}| \sin(\theta) + \right. \right. \\ \left. \left. + \mathbf{n} |\Lambda \mathbf{z}|^2 (3 \sin^2(\theta) - 1) \right] \right\} \quad (30)$$

to within terms that are linear in the parameter kR_0 (the near-field approximation); θ is the angle, at which the point of observation is seen (see Fig. 1). Therefore, the size and the shape of the emitting particle affect the photon emission through the integration over the particle's volume and due to the presence of the local-field factor.

The radiation pattern for the emitted energy of the electromagnetic field is

$$\frac{d\bar{I}}{d\Omega} = \mathbf{n} \mathbf{S} R^2 = (\omega I_0)^2 \times \\ \times \int_V d\mathbf{R}' \frac{R^2}{R_0^5} \left[|\Lambda \mathbf{z}|^2 (3 \sin^2(\theta) - 1) - 2\mathbf{n}(\Lambda \mathbf{z}) |\Lambda \mathbf{z}| \sin(\theta) \right]. \quad (31)$$

This expression will be basic for numerical calculations of radiation patterns of the emitted energy at fixed distances from the particle center.

5. Numerical Calculations

To illustrate the developed approach, we calculated radiation emission patterns for extended cubic particles. A mesoparticle and a quantum dot were considered. The results of numerical calculations are presented graphically, where the distance from the coordinate origin to a point at the calculated surface in the three-dimensional space corresponds to the electromagnetic field energy emitted by the particle (in relative units). The radiated field energy was calculated on the sphere with radius R , and the direction from the coordinate origin to the point of observation was given by the vector \mathbf{R} direction (see Fig. 1). The coordinate origin was fixed at the center of the cubic particle. The axes of the coordinate system pass through the centers of cube faces. The results of calculations are presented separately for a mesoparticle (when the effects of spatial quantization are insignificant) and for a quantum dot.

Let us consider a cubic mesoparticle with the edge length $a = 1 \times 10^{-6}$ m, and let the dielectric permittivity of its material be equal to 11. The radiation patterns were calculated by formula (31) for various distances from the particle's center. The calculation results revealed a strong dependence of radiation patterns on the distance R from the particle's center to the point of observation that is located on a sphere with radius R . At short distances, the radiation pattern was strongly anisotropic. It was composed of narrow lobes directed along the spatial diagonals of the cube (Figs. 2 and 3). As the distance R (the radius of observation sphere) increased, the lobes became strongly deformed (Fig. 4,a), and, at distances longer than $3R$, the radiation pattern was almost indistinguishable from that of a point dipole (Fig. 4,b).

It should be noted that, for simplicity, we supposed the material that the mesoparticle was made of as such that only oscillations of electric dipoles directed along the axis OZ gave contributions to the radiation induction. Therefore, the radiation pattern symmetry is uniaxial at large enough distances between the particle and the point of field observation. It is of interest to monitor the variation of the spatial shape of the radiation pattern as the radius of observation sphere

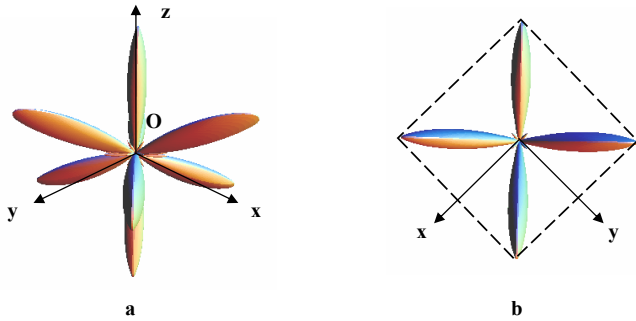


Fig. 2. Radiation pattern of a cubic mesoparticle at $R = 1.5a$. (a) General view and (b) top view (along the OZ axis). The distance from an arbitrary point on the lobe surface to the frame origin gives the magnitude of the field energy flux in this direction

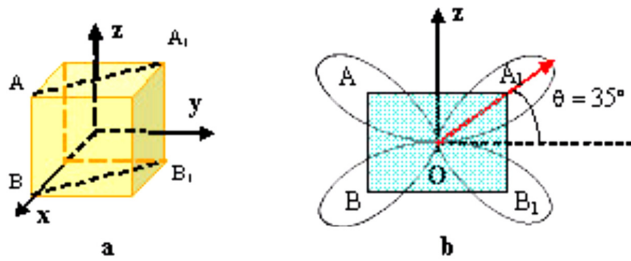


Fig. 3. (b) Cross-section of the field energy flux emitted by a cubic mesoparticle in the plane AA_1B_1B formed by two intersecting diagonals of the cube (a)

grows. First, the lobes get smeared and merged into two rounded square “half-bowls” joined at their bases (see Fig. 4,a). As the radius of the observation sphere increases, the radiation pattern becomes more and more symmetric and dome-shaped. At distances more than $3R$ from the particle, it emits as a point dipole.

Similar results were obtained for the light emission by a quantum dot. In this work, the main attention was focused on studying the influence of the emitting particle’s extension on the formation of a radiation pattern of the electromagnetic field energy flux. Therefore, we considered the simplest case of a cubic quantum dot in the uniform isotropic medium. Namely, a GaAs quantum dot was considered, for which the effective electron mass was $m_e = 0.068 m_0$, where m_0 is the free electron mass. As the medium, $Ga_{1-x}Al_xAs$ was selected, which emits light with the photon energy $\hbar\omega_0 \approx 1$ eV. The damping constant ν was selected to provide the equality $\hbar\nu \approx 0.05\hbar\omega_0$. The conduction electron density was taken $n_e = 10^{18} \text{ cm}^{-3}$. Therefore,

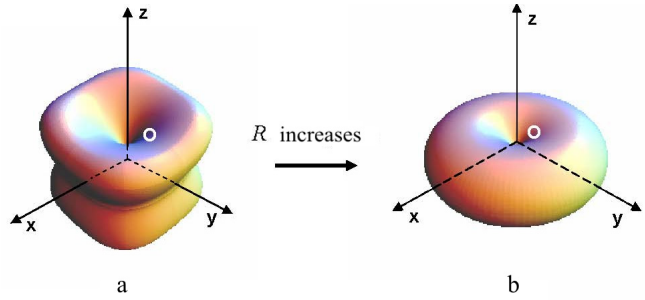


Fig. 4. Radiation patterns of the light emission by a cubic mesoparticle at the distances $R = 2.5a$ (a) and $R = 3a$ (b)

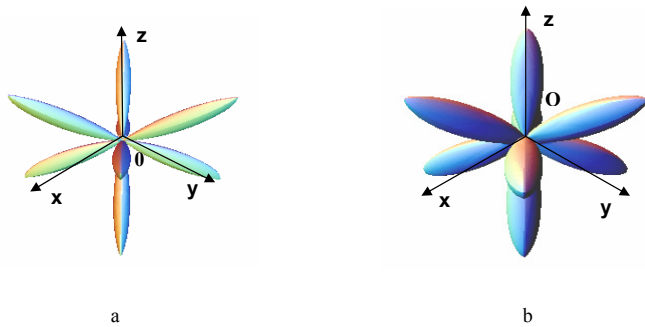


Fig. 5. Radiation patterns of the electromagnetic field energy flux emitted by a quantum dot at $R = 1.5a$ (a) and $R = 2.5a$ (b)

provided that the cube edge length was $a = 12$ nm, the particle included two conduction electrons. When calculating the linear response to the local field by formula (12), we made allowance for transitions between the ground (111) and two excited states that corresponded to the excitation of electron currents directed along the OZ axis [36], namely, $(111) \rightarrow (112)$ with the energy $\varepsilon_{nm} = 0.15$ eV and $(111) \rightarrow (114)$ with the energy $\varepsilon_{nm} = 0.76$ eV. As a result, we obtained the radiation patterns that were very similar to those calculated for a mesoparticle. At short distances from the quantum dot ($R = 1.5a$ and $R = 2.5a$), the radiation patterns for the quantum dot look as shown in Fig. 5. The increase of the distance to $R = 3.5a$ is accompanied by a deformation of the radiation pattern toward the radiation pattern of a point dipole. That is, the influence of the particle’s extension on the formation of the radiation pattern of a quantum dot is observed at short distances from the particle, as it was in the mesoparticle case.

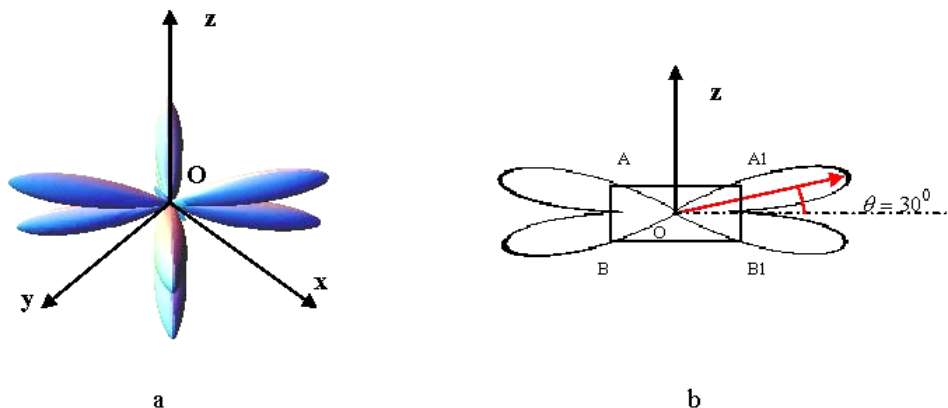


Fig. 6. Radiation pattern of the electromagnetic field energy flux emitted by a $17 \times 17 \times 6.8418\text{-nm}^3$ quantum dot: (a) general view and (b) its cross-section at the distance $R = 1.5 \times 17.1 \text{ nm} = 25.65 \text{ nm}$

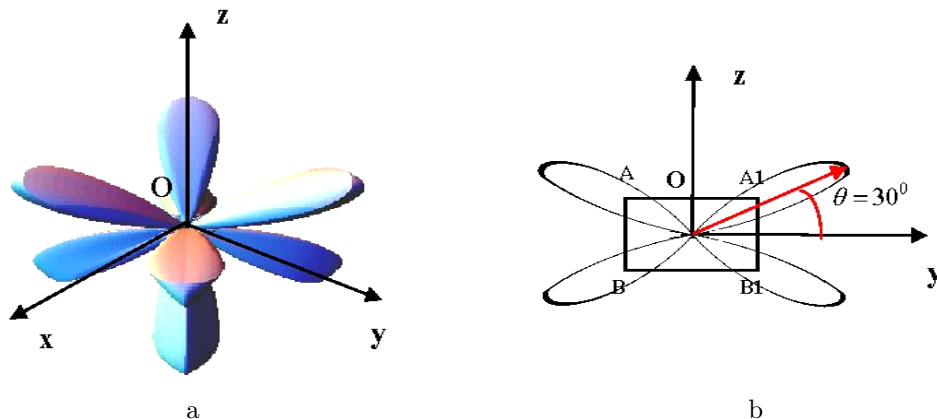


Fig. 7. Radiation pattern of the electromagnetic field energy flux emitted by a mesoparticle $a \times a \times 0.4a$ ($a = 10^{-6} \text{ m}$) in dimension: (a) general view and (b) its cross-section at the distance $R = 1.5 \times 10^{-6} \text{ m}$

6. Conclusions

In this paper, we have considered the influence of particle extension effects on the spontaneous photon emission by a nanoparticle. Two cases were examined: the spontaneous light emission by a mesoparticle – a particle, in which the spatial quantization effects are insignificant – and a quantum dot. In order to study the particle’s extension effects, we have modified the theory proposed earlier by one of the authors (O.K.) [19–21]. The theory was improved by including the self-field (local-field) effects on the oscillating dipole of electron transitions in a particle under consideration. The self-field was found by solving a self-consistent equation – the Lippmann–Schwinger equation – for the local field. The equations for particles of both kinds, a mesoparticle and a quantum dot, were solved in the

framework of the concept of effective susceptibility. An analytic expression for the field energy flux emitted by the particle has been obtained. This expression was used in numerical calculations of radiation patterns for the spontaneous emission by a cubic particle. At short distances from the particle’s center, the radiation patterns for a mesoparticle and a quantum dot look like narrow lobes directed along the spatial diagonals of the cube. The almost identical shapes of the radiation patterns for a quantum dot and a mesoparticle can be explained by the fact that the radiation pattern is almost independent of the spectrum in the near-field zone, being mainly governed by the geometric shape of a particle. To confirm this conclusion, we made relevant calculations for a mesoparticle and a quantum dot, both plate-like, $a \times a \times 0.4a$ ($a = 10^{-6} \text{ m}$) and $17.1 \times 17.1 \times 6.8418 \text{ nm}^3$ in dimension,

respectively. The results are depicted in Figs. 7 and 6, respectively.

The increase of the distance to the observation sphere is accompanied by a smearing of those lobes and a transformation of the radiation pattern: at distances $R \geq 2a$ for a mesoparticle and $R \geq 3.5a$ for a quantum dot, the corresponding radiation pattern practically does not differ from that of a point dipole. This fact can serve as a substantiation of the statement that two nanoparticles located at a distance more than a few of their linear dimensions interact with each other as point dipoles. This means that the results obtained here can serve as an indirect substantiation of the validity of quasipoint dipole model which is widely used in the framework of the electro-dipole approximation for the explanation of a good many effects in submonolayer molecular coatings on the surfaces of solids.

1. V.V. Mitin, V.A. Kochelap, and Strosio M.A.. *Quantum Heterostructures* (Cambridge University Press, Cambridge, 1998).
2. *Physics of Low-Dimensional Semiconductor Structures*, edited by P. Butcher, N.H. March, and M.P. Tosi (Plenum Press, New York, 2001).
3. M. Geissler and Y. Xia, *Adv. Matter* **16**, 1249 (2004).
4. N.N. Gerasimenko, *Russ. Khim. Zh.* **46**, N 5, 30 (2002).
5. O. Keller, *Phys. Rep.* **268**, 85 (1996).
6. C. Girard, C. Joachim, and S. Gauthier, *Rep. Prog. Phys.* **63**, 893 (2000).
7. Ch. Girard and A. Dereux, *Rep. Prog. Phys.* **59**, 657 (1996).
8. R.C. Dunn, *Chem. Rev.* **99**, 2891 (1999).
9. A.V. Zayats, I.I. Smolyaninov, and A.A. Maradudin, *Phys. Rep.* **408**, 131 (2005).
10. S. Pataene, P.G. Gucciardi, M. Labardi and M. Allegrini, *Riv. Nuovo Cimento* **27**, 1 (2004).
11. A.N. Grigirenko, A.K. Geim, H.F. Gleeson *et al.*, *Nature* **438**, 335 (2005).
12. R.D. Schaller, J.C. Johnson, K.R. Wilson *et al.*, *J. Phys. Chem. B* **106**, 5143 (2002).
13. J.-C. Weeber, J.R. Krenn, A. Dereux *et al.*, *Phys. Rev. B* **64**, 045411 (2001).
14. B. Hecht, B. Sick, U. Wild *et al.*, *J. Chem. Phys.* **112**, 7761 (2000).
15. J. Tominaga, C. Michalcea, D. Buchel *et al.*, *Appl. Phys. Lett.* **78**, 2417 (2001).
16. B. Rosner and D.W. van der Weide, *Rev. Sci. Instrum.* **73**, 2505 (2002).
17. O. Keller, *Phys. Rev. A* **62**, 022111 (2000).
18. T. Inoue and H. Hori, *Quantum Theory of Radiation in Optical Near Field Based on Quantization of Evanescent Electromagnetic Waves Using Detector Mode* (Springer, Berlin, 2005).
19. O. Keller, *J. Chem. Phys.* **112**, 7856 (2000).
20. O. Keller, *Phys. Rev. A* **76**, 062110 (2007).
21. O. Keller, *Phys. Rev. A* **62**, 022111 (2000).
22. C.J. Orendorff, T.K. Sau, and C.J. Murphy, *Small* **2**, 636 (2006).
23. A.V. Goncharenko, V.Z. Lozovski, and E.F. Venger, *J. Phys.:Condens. Matter* **13**, 8217 (2001).
24. B.F. Soares, K.F. MacDonald, and N.I. Zheludev, in *Abstracts of the International Quantum Electronics Conference (IQEC-2004)*, p. 838.
25. T. Jensen, L. Kelly, A. Lazarides, and G.C. Schatz, *J. Cluster Sci.* **10**, 295 (1999).
26. S. Bozhevolnyi and V. Lozovski, *Phys. Rev. B* **61**, 11139 (2000).
27. V. Lozovski, Yu. Nazarov, and S.I. Bozhevolnyi, *Physica E* **11**, 323 (2001).
28. S.I. Bozhevolnyi and V. Lozovski, *Phys. Rev. B* **65**, 235420 (2002).
29. A.A. Abrikosov, L.P. Gor'kov, and I.E. Dzyaloshinskij, *Methods of Quantum Field Theory in Statistical Physics* (Prentice Hall, Englewood Cliffs, 1963).
30. L. Knöll, S. Scheel, and D.-G. Welsch, in *Coherence and Statistics of Photons and Atoms*, edited by J. Petina (Wiley, New York, 2001), p. 1.
31. L.D. Landau and E.M. Lifshitz, *Quantum Mechanics. Non-Relativistic Theory* (Pergamon Press, New York, 1965).
32. S. Flügge, *Practical Quantum Mechanics* (Springer, New York, 1974).
33. O. Keller, *J. Quant. Nonlinear Phenom.* **1**, 139 (1992).
34. V. Lozovskii, *Opt. Spektrosk.* **86**, 107 (1999).
35. O. Keller, M. Xiao, and S. Bozhevolnyi, *Opt. Commun.* **114**, 491 (1995).
36. O. Keller and T. Garm, *Physica Scripta* **54**, 115 (1994).
37. N. Budkova and V. Lozovskii, *Ukr. Fiz. Zh.* **45**, 225 (2000).
38. L.D. Landau and E.M. Lifshits, *The Classical Theory of Fields* (Pergamon Press, Oxford, 1983).

Received 19.03.08.

Translated from Ukrainian by O.I. Voitenko

ВПЛИВ ЕФЕКТІВ ЛОКАЛЬНОГО ПОЛЯ НА СПОНТАННУ ЕМІСІЮ ФОТОНІВ НАНООБ'ЄКТАМИ

I. Єжокін, О. Келлер, В. Лозовський

Резюме

На основі методу локального поля побудовано схему розрахунків діаграм направленостей наночастинками різної форми. Основна ідея методу полягає в побудові самоузгоджених рівнянь для електромагнітного поля в довільній точці системи. Розв'язок рівнянь дає співвідношення, що пов'язують локальне поле в довільній точці системи з зовнішнім довгохвильовим полем через фактор локального поля. Фактор локального поля дає зв'язок між затравочним моментом оптичного дипольного переходу одиниці об'єму системи та ефективним дипольним моментом переходу з урахуванням ефектів локального поля. Цей ефективний дипольний момент залежить від форми та

розміру частинки. В результаті випромінення такого диполя залежить від форми та розміру частинки. В роботі розраховано діаграми направленості випромінення частинками кубічної форми та показано, що на відстанях, які перевершують ліній-

ні розміри об'єктів, частинки взаємодіють майже як точкові диполі. Це може, зокрема, слугувати обґрунтуванням застосування електродипольного наближення для вивчення оптичних властивостей субмоношарових молекулярних покриттів.